Intermittency as a consequence of turbulent transport in nonlinear systems

Benno Rumpf*

Max-Planck-Institute for the Physics of Complex Systems, Nöthnitzer Strasse 38, 01187 Dresden, Germany

Alan C. Newell

Mathematics Department, University of Arizona, Tucson, Arizona 85721

Intermittent high-amplitude structures emerge in a damped and driven discrete nonlinear Schrödinger equation whose solutions transport both energy and particles from sources to sinks. These coherent structures are necessary for any solution that has statistically stationary transport properties.

Turbulent flow that transfers energy from a stirring range at large scales to the dissipation range at small scales consists of dissimilar components, a broad spectrum of eddies and randomly occurring, intermittent coherent structures. The first cascade leads to Kolmogorov-like finite-flux power spectra. The second component is particularly visible in the anomalous short-scale behavior of the higher order moments of velocity differences. Compared to fully developed three-dimensional turbulence, it is easier to quantify these two components in turbulent systems of weakly coupled dispersive waves. In this case, the Kolmogorov-Zakharov spectrum is a stationary finite flux solution of kinetic equations that follow from three and four wave resonances of weak interactions. The second component emerges since the wave turbulence approximation [1] is almost never valid at very low and very high wave numbers where the "weak" coupling approximation breaks down, and leads to the emergence of fully nonlinear structures [2]. In short, despite the fact that the amplitudes are, on average, small, the weakly nonlinear dynamics can lead to intermittent localized high-amplitude events and anomalies in high order moments. It may also lead to contamination of low order moments and to power spectra which, at least in some wave number ranges, are dominated by strongly nonlinear events. Nowhere is this more evident than in the illuminating studies of Cai, Majda, McLaughlin, and Tabak (CMMT) [3] (later confirmed by Zakharov *et al.* [4]) on damped, driven and freely decaying weakly nonlinear dispersive one-dimensional wave systems. Indeed, CMMT found that, in damped and driven systems, there were some situations in which the nonlinear solutions dominated at almost all scales. In the freely decaying state, they found that Kolmogorov-Zakharov spectra were much more likely to appear. This of course was disappointing because the strength of the Kolmogorov-Zakharov solution of the undamped, undriven kinetic equation is that it describes exactly what would be expected if an energy source at $k=0$ feeds at a constant flux rate through an inertial range to a viscous sink at $k=\infty$.

The purpose of this paper is to demonstrate in a simple but representative model that in driven, damped systems in which there are fluxes of two conserved densities (energy

and particle number), realization of a *statistically steady* state demands the existence of high-amplitude coherent structures because they play a crucial role in balancing the energy flux budget. We show that a single cascade of weakly interacting waves that transport particles from a source to a sink leads to a steady net loss of energy in the system. Any steady solution requires contributions from the nonlinear terms in order to offset this loss in energy. This is achieved by intermittent formation and destruction of high-amplitude structures. Figure 1 shows the intermittent emergence of peaks for a discrete nonlinear Schrödinger equation,

$$i\dot{\phi}_n + \phi_{n+1} + \phi_{n-1} - 2\phi_n + \phi_n^2\phi_n^* = \mathcal{F}(\phi,t) - \mathcal{D}(\phi,t),$$
(1)

for a chain of complex oscillators. $\mathcal{D}$ is a short-wavelength damping term whereas $\mathcal{F}$ drives the system on long space scales. Figure 1(a) displays the typical long-time behavior of $|\phi_n|^2$ in a sector of 30 lattice sites from a chain of $N=512$ oscillators with periodic boundary conditions over 30 time units. $|\phi_n|^2$ is small on average, but high-amplitude structures emerge locally. The peak shows "breathing" behavior, which decreases and increases irregularly. Figure 1(b) shows the average density ρ of oscillators with amplitude $|\phi|$ for weak and for strong damping forces. The density for small
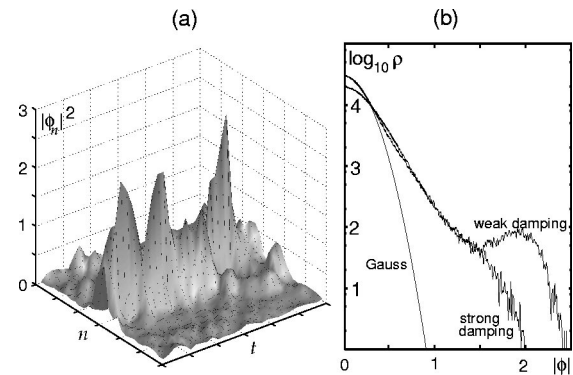

FIG. 1. Numerical integration of the damped and driven discrete nonlinear Schrödinger equation: (a) $|\phi_n|^2$ for a sector of 30 oscillators over 30 time units with strong damping. (b) Density of sites with amplitude $|\phi|$ as a function of $|\phi|$ for weak and for strong damping and a Gaussian fit of the density for weak damping.

---

*Email address: benno@mpipks-dresden.mpg.de

$|\phi|$ is Gaussian, but for larger $|\phi|$ the intermittent high-amplitude structures lead to slower non-Gaussian decay. In the weakly damped system, the density increases slightly for high amplitudes so that there is a small hump near $|\phi|=2$. The number of these intermittent events increases with the driving force, but the hump remains in the vicinity of $|\phi|=2$.

In the simulations we use time-periodic δ kicks as damping and driving forces $\mathcal{D}$ and $\mathcal{F}$, which allows a simple control of the energy input and output: The driving increases the homogeneous mode $c_0 \to (1+\lambda_{\mathcal{F}})c_0$, and the damping decreases modes on a short space scale like $c_k \to (1-\lambda_{\mathcal{D}})c_k$ where $c_k = (1/N)\Sigma_n \phi_n \exp(ikn)$ and wave number k is in the Brillouin zone $[0,2\pi]$. In numerical studies we apply damping to the short-wavelength modes with $7\pi/8 \leq k \leq 9\pi/8$, so that the impact of damping does not decrease according to the size of the system. Analytical studies are simplified by restricting damping to mode $k=\pi$. $\mathcal{D}$ and $\mathcal{F}$ are zero in the intervals of one time unit between the time-periodic kicks. No important changes are found for shorter intervals between the kicks, or for continuous driving and damping.

The dynamics between the kicks are governed by the nonlinear Schrödinger equation that is derived as $i\dot{\phi}_n = \partial H/\partial \phi_n^*$ from the Hamiltonian,

$$H = H_2 + H_4$$
$$= \sum_n 2\phi_n \phi_n^* - \phi_n \phi_{n+1}^* - \phi_n^* \phi_{n+1} - \frac{1}{2}\sum_n \phi_n^2 \phi_n^{*2}.$$
$$(2)$$

The modulus square norm or particle number,

$$A = \sum_n \phi_n \phi_n^* = N\sum_k c_k c_k^*,$$
$$(3)$$

is a second quantity that is conserved. In recent studies [5] we have shown that this isolated Hamiltonian system with no damping and driving force forms localized high-amplitude structures as a statistical consequence of thermalization under constraint of its two *conserved* quantities. These peaks are generated in a self-focusing process of low-amplitude waves with long wavelengths and low energy. A typical initial condition from which high-amplitude peaks emerge is the Rayleigh–Jeans distribution of power $|c_k|^2 = [\beta(\omega(k)+\gamma)]^{-1}$ with positive temperature β^{-1}. γ is the chemical potential, and $\omega(k)=2-2\cos k$ is the frequency. As the system approaches its state of maximum entropy, the spectrum of low-amplitude fluctuations becomes flat so that the power is equipartitioned on all modes ($\beta \to 0, \gamma \to \infty$). During this transformation of the low-energy spectrum to an equipartitioned spectrum, stable high-amplitude peaks with negative energy emerge as a by-product of the production of entropy in the low-amplitude waves. No such peaks emerge from low-amplitude short waves with high energy.

In contrast, the long time behavior of solutions of the damped and driven system is governed, not by the values of H and A, but by the *fluxes* of both quantities. Each driving step $\mathcal{F}$ changes amplitude ϕ_n by $\Delta \phi_n = \lambda_{\mathcal{F}}c_0$, so that the total number of particles increases by $\Delta_{\mathcal{F}}A = \Sigma_n \phi_n \Delta \phi_n^*$
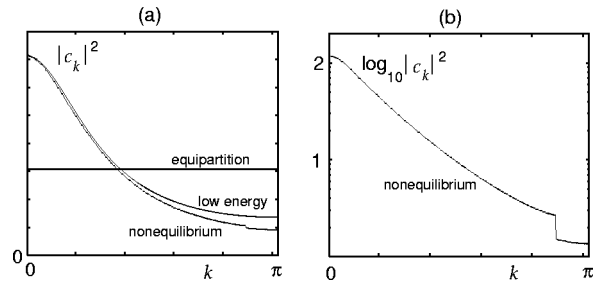

FIG. 2. (a) Spectrum of a weakly damped nonequilibrium system compared to a similar low-energy thermodynamic spectrum $[\beta(\omega(k)+\gamma)]^{-1}$ of the corresponding undamped undriven Hamiltonian system. (b) Logarithmic plot of the spectrum for strong damping. The steps of the spectra at $k=7\pi/8$ result from damping.

$+\Delta \phi_n \phi_n^* = 2\lambda_{\mathcal{F}}N|c_0|^2$ while the damping changes the particle number by $\Delta_{\mathcal{D}}A = -2\lambda_{\mathcal{D}}N|c_\pi|^2$ for small values of $\lambda_{\mathcal{F},\mathcal{D}}$. Consequently, there is a flow of particles from the source at $k=0$ to the sink at $k=\pi$, and the power spectrum [Fig. 2(a)] decays according to the wave number. With most power gathered at low wave numbers, the spectrum is similar to a thermodynamic spectrum [Fig. 2(a)] of the corresponding undamped undriven Hamiltonian system with low energy. The high-amplitude structures are generated by the same mechanism in such an isolated Hamiltonian system and in the damped driven system where the permanent particle flow maintains the bias of the spectrum. The spectrum decays even exponentially for strong damping forces Fig. 2(b). Particle loss and gain are balanced when the flow in a sufficiently large system is constant so that

$$\Delta_{\mathcal{F}}A + \Delta_{\mathcal{D}}A = 0,$$
$$(4)$$

or $\lambda_{\mathcal{F}}|c_0|^2 = \lambda_{\mathcal{D}}|c_\pi|^2$. The driving parameter $\lambda_{\mathcal{F}}$ and the damping parameter $\lambda_{\mathcal{D}}$ regulate the particle number and the particle flux of the system. By choosing the driving parameter as $\lambda_{\mathcal{F}} = \Delta A/2N|c_0|^2$ we obtain a constant flow of particles, $\Delta_{\mathcal{F}}A = \Delta A$, into the system in the numerical simulations. Damping parameter $\lambda_{\mathcal{D}}$ is fixed. For a strong damping to forcing ratio, $\lambda_{\mathcal{D}} = \epsilon^{-2}\lambda_{\mathcal{F}}$ with $\epsilon^2 \ll 1$, it follows from Eq. (4) that $|c_\pi| = \epsilon|c_0|$ and

$$\lambda_{\mathcal{F}}|c_0| = \epsilon \lambda_{\mathcal{D}}|c_\pi|.$$
$$(5)$$

The input and output of particles also change the quadratic coupling energy and the quartic energy. Gains and losses again have to match in a stationary nonequilibrium state so that

$$\Delta_{\mathcal{F}}H_2 + \Delta_{\mathcal{F}}H_4 + \Delta_{\mathcal{D}}H_2 + \Delta_{\mathcal{D}}H_4 = 0.$$
$$(6)$$

In order to understand the role of the strongly nonlinear terms in energy flow, we analyze how it is divided among these four terms. The change in quadratic coupling energy, $H_2 = N\Sigma \omega(k)c_k c_k^*$, is given by the flux of particles times frequency $\omega(k)$. The influx of particles through the driving force leads to zero energy influx, $\Delta_{\mathcal{F}}H_2 = \omega(0)\Delta A = 0$, since $\omega(0)=0$. The damping leads to loss of coupling energy, $\Delta_{\mathcal{D}}H_2 = -\omega(\pi)\Delta A$, with $\omega(\pi)=4$. Consequently, the par-
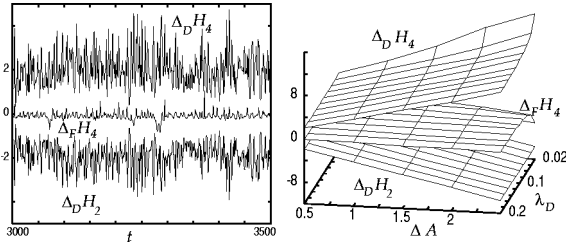
FIG. 3. (a) Change of H_2 due to damping and of H_4 due to damping and the driving force as a function of time. (b) Time average of the same energy flows as a function of the particle flow ΔA and the damping constant $\lambda_{\mathcal{D}}$.

ticle flux leads to a net loss of coupling energy of $\Delta H_2 = \Delta_{\mathcal{F}} H_2 + \Delta_{\mathcal{D}} H_2 = -4\Delta A$. This loss in energy must be balanced by a gain in energy in the nonlinear term H_4 to maintain a stationary state of nonequilibrium. The viscosity changes nonlinear energy $H_4 = -(1/2)\Sigma \phi_n^2 \phi_n^{*2}$ as

$$\Delta_{\mathcal{D}} H_4 = 2\lambda_{\mathcal{D}} N Re(d_\pi c_\pi^*),$$

where $d_k = (1/N)\Sigma_n |\phi_n|^2 \phi_n e^{ikn}$. Driving changes this energy contribution by

$$\Delta_{\mathcal{F}} H_4 = -2\lambda_{\mathcal{F}} N Re(d_0 c_0^*).$$

Figure 3(a) shows $\Delta_{\mathcal{D}} H_2$, $\Delta_{\mathcal{F}} H_4$ and $\Delta_{\mathcal{D}} H_4$ as functions of time for a chain of 512 oscillators for a total particle flux per time unit of $\Delta A = 0.512$ and a strong damping to forcing ratio where $\lambda_{\mathcal{D}} = 0.2$. This corresponds to the simulation in Fig. 1(a), the strong damping case in Figs. 1(b) and 2(b) and to Figs. 4(c) and 4(d). The fluctuations indicate single collapse events which have smaller relative strength for larger size systems. Figure 3(b) shows the time average of $\Delta_{\mathcal{D}} H_2$, $\Delta_{\mathcal{F}} H_4$, and $\Delta_{\mathcal{D}} H_4$ as functions of damping coefficient $\lambda_{\mathcal{D}}$ and particle flux ΔA, whereas the weakly driven case ($\Delta A = 0.512$) corresponds to that in all other simulations. The impact of the driving force on energy $\Delta_{\mathcal{F}} H_4 \approx 0$ is negligible compared to the two effects of damping, $\Delta_{\mathcal{D}} H_2$ and $\Delta_{\mathcal{D}} H_4$.
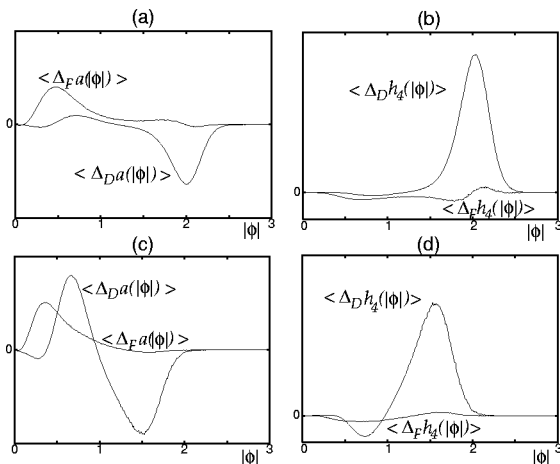

FIG. 4. Average loss and gain of particles [(a) and (c)] and of nonlinear energy [(b) and (d)] as functions of the amplitude $|\phi|$. (a),(b) Weak damping case; (c),(d) strong damping case.

This predominance of $\Delta_{\mathcal{D}} H_4$ over $\Delta_{\mathcal{F}} H_4$ [i.e., $\lambda_{\mathcal{F}} Re(d_0 c_0^*) \ll \lambda_{\mathcal{D}} Re(d_\pi c_\pi^*)$] follows from $\lambda_{\mathcal{F}}|c_0| \ll \lambda_{\mathcal{D}}|c_\pi|$ according to Eq. (5) and from $|d_\pi| \sim \mathcal{O}(|d_0|)$. The second relation is due to the spiky shape of $|\phi_n|^2 \phi_n$ that leads to a flat power spectrum. In addition, the phases of d_π and c_π are correlated by the phase velocity of the peaks while $d_0 c_0^*$ oscillates randomly since it is governed by low-amplitude fluctuations. $\Delta_{\mathcal{F}} H_4$ yields a significant negative contribution only for high particle flux ΔA and weak damping force $\lambda_{\mathcal{D}}$ [at $\lambda_{\mathcal{D}} = 0.02$, $\Delta A = 2.5$ in Fig. 3(b)].

For all other cases, both $\Delta_{\mathcal{F}} H_2$ and $\Delta_{\mathcal{F}} H_4$ are zero or close to zero, so Eq. (6) reduces to $\Delta_{\mathcal{D}} H_2 \approx -\Delta_{\mathcal{D}} H_4$. This yields $Re(c_\pi^* d_\pi) \approx 4 c_\pi^* c_\pi$ or the inequality,

$$|d_\pi| \gtrsim 4|c_\pi|. \tag{7}$$

The importance of nonlinearity $\Delta_{\mathcal{D}} H_4$ in the balance of energy is reflected in the system's first three moments: By defining $\psi_n = \phi_n(-1)^n$, the inequality, Eq. (7), reads $|\Sigma|\psi_n|^2 \psi_n| \gtrsim 4|\Sigma \psi_n|$. The first moment $|\Sigma \psi_n| \sim \sqrt{\Delta A}$ increases with the particle flux. The second moment $\Sigma|\psi_n|^2 = A$ is the particle number, which is small if the system is strongly damped and weakly driven. Equation (7) shows that the third moment exceeds the first moment, so the distribution is strongly non-Gaussian. High-amplitude excitations [Fig. 1(a)] that lead to the non-Gaussian tails in Fig. 1(b) are necessary to maintain a stationary state of nonequilibrium under the flow of energy and particles.

To understand how the high-amplitude structures balance the energy flow, we compute the input and output of energy and particles as functions of the amplitude $|\phi|$ of the oscillators. The driving kick feeds a number $\Delta_{\mathcal{F}} a(|\phi|)d|\phi| = \Sigma_{n:|\phi| \leqslant |\phi_n| \leqslant |\phi| + d|\phi|} 2Re(\phi_n \Delta_{\mathcal{F}} \phi_n^*)$ of particles to those lattice sites where the amplitude is between $|\phi|$ and $|\phi| + d|\phi|$. The total particle gain used in Eq. (4) is $\Delta_{\mathcal{F}} A = \int_0^\infty \Delta_{\mathcal{F}} a(|\phi|)d|\phi|$. Similarly, the forcing changes the nonlinear energy at these lattice sites by $\Delta_{\mathcal{F}} h_4(|\phi|)d|\phi| = \Sigma_{n|\phi| \leqslant |\phi_n| \leqslant |\phi| + d|\phi|} 2|\phi_n|^2 Re(\phi_n^* \Delta_{\mathcal{F}} \phi_n)$. The increments in damping $\Delta_{\mathcal{D}} a(|\phi|)$ and $\Delta_{\mathcal{D}} h_4(|\phi|)$ are defined analogously. $\Delta_{\mathcal{F}} h_2(|\phi|)$ is again zero, and $\Delta_{\mathcal{D}} h_2(|\phi|) = \omega(\pi)\Delta_{\mathcal{D}} a(|\phi|)$. Figure 4 shows the time average of the influx and outflux of particles and energy as functions of $|\phi|$. In the weakly damped case [Figs. 4(a) and 4(b)] with $\lambda_{\mathcal{D}} = 0.02$ and $\Delta A = 0.512$]. The particles are fed into the system mainly at those lattice sites where the amplitude is moderate [$|\phi| \approx 0.5$ in Fig. 4(a)], while particles are removed mainly at sites with high amplitudes of $|\phi| \approx 2$. While the input of particles has a negligible effect on the balance of nonlinear energy, the output of particles leads to a gain in energy that peaks at $|\phi| \approx 2$. Remarkably, a very small number of sites with high amplitudes is responsible for practically the total outflux of particles and the corresponding feedback of nonlinear energy.

This gain in energy can be seen for the most simple case of an isolated real peak, $\phi_n = \chi \delta_{nl}$, whose height decreases by $\Delta_{\mathcal{D}} \phi = \lambda_{\mathcal{D}} c_\pi \ll \chi$ during the damping kick, so the coupling energy changes by $\Delta_{\mathcal{D}} H_2 = -8\chi\Delta_{\mathcal{D}}\phi$. This increases the nonlinear energy by $\Delta_{\mathcal{D}} H_4 = 2\chi^3 \Delta_{\mathcal{D}}\phi$. The fluxes are

balanced if the peak amplitude is $\chi = 2$, which agrees with the results of Figs. 4(a) and 4(b). Particles removed from the tip of the peak have to be replaced constantly through the driving mode at $k = 0$. During Hamiltonian evolution, the focusing process increases the peak again while short-wave fluctuations are radiated.

The input of particles in the strongly damped equation [Figs. 4(a) and 4(b) with $\lambda_{\mathcal{D}} = 0.2$, $\Delta A = 0.512$] is maximal for low amplitudes of $|\phi| \approx 0.4$, similar to in the weakly damped case in Fig. 4(a). Damping leads to a significant loss of particles at $|\phi| \approx 1.5$, and to a tiny loss of particles in the domain of low-amplitude fluctuations at $|\phi| \approx 0.2$, but, paradoxically, also to particle gain at $|\phi| \approx 0.7$. While there is still a net loss of particles, this partial recycling of particles increases the ratio of energy gain per particle loss. This allows the system to satisfy the balance condition, Eq. (7), with a peak amplitude less than $|\phi| = 2$. As a simple model for this mechanism we assume two peaks at sites l and $l+3$ where $\phi_l = \chi > \xi = \phi_{l+3}$ are real and positive. A damping kick decreases the higher peak to $\phi_l = \chi - \Delta_{\mathcal{D}}\phi$ and increases the lower peak to $\phi_{l+3} = \xi + \Delta_{\mathcal{D}}\phi$. The decrease of the higher peak ϕ_l models the particle loss at $|\phi| \approx 1.5$ in Fig. 4(c) and the increase of the lower peak ϕ_{l+3} represents the gain of particles at $|\phi| \approx 0.7$. The coupling energy loss is $\Delta_{\mathcal{D}}H_2 = -8(\chi - \xi)\Delta_{\mathcal{D}}\phi$ and the nonlinear energy gain is $\Delta_{\mathcal{D}}H_4 = 2(\chi^3 - \xi^3)\Delta_{\mathcal{D}}\phi$. The gain of nonlinear energy can outweigh the loss of coupling energy for $\chi > 2/\sqrt{3}$.

In summary, coherent structures are an essential component of the transport of particles from large scales to small dissipation scales. The particle flow leads to a steady loss of coupling energy, so the fluctuations have a low ratio of energy per particle. Such long-wave fluctuations form high-amplitude structures [5], and it is the role of coherent structures to balance the energy input and output by exploiting the nonlinear component of the energy. To offset this loss in energy, high-amplitude structures that contain a significant amount of negative nonlinear energy must be formed and destroyed. Energy is transferred from nonlinearity H_4 to coupling H_2 during peak growth, and pruning or destroying the peaks increases the system's total energy. The peaks are essentially the pipes through which energy and particles flow under the constraints of balance conditions.

Obviously, this effect follows purely from the dispersion and the nonlinearity, and it is not restricted to the one-dimensional discrete system of our simulations. Similar behavior was found [2] for the two-dimensional continuous focusing nonlinear Schrödinger equation when force is applied at a midrange wave number and damping at large wave numbers. This leads to energy flux toward high wave numbers, and to inverse particle flux to low wave numbers. The particle flux builds condensates from which collapsing solitons emerge that carry particles to the dissipation scale and feed both particles and energy back into the wave field at these high wave numbers. With almost Gaussian statistics of the waves and Poisson distribution of the intermittent coherent events, the system resembles a two species gas. The presence of collapses does not appear to affect low moment statistics of two- or three-dimensional systems if the damping is sufficiently strong, whereas collapses contaminate the power spectrum generated by wave–wave interaction in nonintegrable one-dimensional systems. The important point to stress is that no particles would be dissipated and no steady state would be achieved without strongly nonlinear collapses.

[1] A.C. Newell, S. Nazarenko, and L. Biven, Physica D **152–153**, 520 (2001); L. Biven, C. Connaughton, and A.C. Newell, *ibid.* **184**, 98 (2003).

[2] S. Dyachenko, A.C. Newell, A. Pushkarev, and V.E. Zakharov, Physica D **57**, 96 (1992); A.C. Newell and V.E. Zakharov, in Turbulence: A Tentative Dictionary, edited by P. Tabeling and O. Cardoso (Plenum, New York, 1995), pp. 59–66.

[3] A.J. Majda, D.W. McLaughlin, and E.G. Tabak, J. Nonlinear Sci. **6**, 9 (1997); D. Cai, A.J. Majda, D.W. McLaughlin, and E.G. Tabak, Physica D **152–153**, 551 (2001).

[4] V.E. Zakharov, P. Guyenne, A.N. Pushkarev, and F. Dias, Physica D **152-153**, 573 (2001).

[5] B. Rumpf and A.C. Newell, Phys. Rev. Lett. **87**, 054102 (2001); Physica D **184**, 162 (2003); B. Rumpf, Phys. Rev. E **69**, 016618 (2004).